Journal of Alloys and Compounds 523 (2012) 182–187

Contents lists available at SciVerse ScienceDirect

Journal of Alloys and Compounds

journal homepage: www.elsevier.com/locate/jallcom

Thermoelectric properties of $Ca_{1-x}Sr_xRuO_3$ compounds prepared by spark plasma sintering

Nittaya Keawprak, Rong Tu*, Takashi Goto

Institute for Materials Research, Tohoku University, Sendai 980-8577, Japan

ARTICLE INFO

Article history:
Received 25 October 2009
Received in revised form 28 January 2012
Accepted 30 January 2012
Available online 7 February 2012

Keywords:
Thermoelectric material
Strontium ruthenate
Calcium ruthenate
Solid solution
Spark plasma sintering

ABSTRACT

Single phase $Ca_{1-x}Sr_xRuO_3$ ($x = 0$–1.0) powders were synthesized by a solid-state reaction and compacted by spark plasma sintering. The *a*-length of the lattice parameter showed a slight minimum around $x = 0.6$, whereas the *b*-length, *c*-length and the unit cell volume increased continuously with increasing *x* from 0 to 1.0, indicating a solid solution in the whole range. The relative density of $Ca_{1-x}Sr_xRuO_3$ compacted bodies increased from 75 to 95% with increasing *x* from 0 to 1.0. The electrical conductivity (σ) at $x = 0.1$–0.9 was higher than those of the end members ($CaRuO_3$ and $SrRuO_3$) except for that at $x = 0.5$, and showed metallic conduction at all compositions. The Seebeck coefficient (*S*) was 30–40 $\mu V K^{-1}$, almost independent of composition and temperature. The thermal conductivity (κ) was 2–3 $W m^{-1} K^{-1}$ at room temperature and increased with increasing temperature. The κ showed the lowest values at $x = 0.2$ in the whole temperature range. The dimensionless figure-of-merit (*ZT*) at $x = 0.1$–0.9 was higher than those of the end members. The highest *ZT* was 0.07 at $x = 0.2$ and 600 K.

1. Introduction

Perovskite-type alkaline-earth metal ruthenium oxides, $ARuO_3$ (A = Ca, Sr and Ba) compounds, show high metallic electrical conductivity associated with *d*-electrons from the three-dimensional network corner-sharing RuO_6 octahedra [1]. $CaRuO_3$ and $SrRuO_3$ are known to be excellent electrical conductors and have been applied as buffer layers in a superconductor-normal metals-superconductor (SNS) Josephson junction [2] and as electrical conducting pastes [3]. Many efforts have been made to reveal the thermodynamic stability [4–6] and magnetic properties [7,8] of $CaRuO_3$ and $SrRuO_3$. Recently, we have prepared $CaRuO_3$ [9–11] and $SrRuO_3$ [12] compacted bodies by spark plasma sintering (SPS) and reported their structural and thermoelectric properties. Table 1 shows comparison of $CaRuO_3$ and $SrRuO_3$ in crystal structure and thermal, electrical and thermoelectric properties [9–12]. $CaRuO_3$ and $SrRuO_3$ have the same crystal structure, i.e., a distorted orthorhombic $GdFeO_3$ type, and the same space group, i.e., *Pnma* [13], and were found to show similar behavior of electrical conductivity (σ), thermal conductivity (κ) and Seebeck coefficient (*S*). In both $CaRuO_3$ and $SrRuO_3$, the σ decreased with increasing temperature, showing metallic behavior. The κ slightly increased with increasing temperature. The *S* was almost independent of temperature and composition, around 25–35 $\mu V K^{-1}$. However, the structure of $CaRuO_3$ is much more distorted than that of $SrRuO_3$ [13,14], which may result in the difference of properties. In our previous study, the lattice parameters of $CaRuO_3$ changed continuously at $R_{Ru/Ca} = 0.7$–1.0, implying a non-stoichiometric range, whereas no solid solution was observed in $SrRuO_3$ [10]. Comparison of σ and κ values at room temperature showed the σ of $SrRuO_3$ single crystals (5×10^5 $S m^{-1}$ at room temperature) [15] to be higher than that of $CaRuO_3$ single crystals (4×10^5 $S m^{-1}$) [16,17]. The σ of an SPS-compacted $SrRuO_3$ polycrystalline body (3.0×10^5 $S m^{-1}$) [12] was also higher than that of $CaRuO_3$ (2.0×10^5 $S m^{-1}$) [9]. The κ of an SPS-compacted $CaRuO_3$ polycrystalline body (3.5–4.0 $W m^{-1} K^{-1}$) was slightly lower than that of $SrRuO_3$ (4.5–6 $W m^{-1} K^{-1}$). The highest dimensionless figure-of-merit (*ZT*) of SPS-compacted $CaRuO_3$ and $SrRuO_3$ polycrystalline body showed almost the same value of 0.025 at 1023 and 600 K, respectively.

In order to improve the thermoelectric properties of $CaRuO_3$ and $SrRuO_3$, κ should be decreased and σ should be increased simultaneously. Kobayashi et al. have reported that the electrical conductivity of the substitution at the Sr^{2+} site by Ca^{2+} ion, i.e., $Ca_{1-x}Sr_xRuO_3$, was higher than those of the end members ($CaRuO_3$ and $SrRuO_3$). The κ of solid solutions is commonly lower than that of the end members. The magnetic properties of $Ca_{1-x}Sr_xRuO_3$ solid solution have been investigated so far, showing that $SrRuO_3$ is a ferromagnet with the critical temperature, $T_c \sim 160$ K. Upon (Sr, Ca) substitution, T_c decreases monotonically with increasing Ca concentration and the ferromagnetic order disappears around $Ca_{0.7}Sr_{0.3}RuO_3$ [18,19]. However, no study on the thermal conductivity and thermoelectric properties of $Ca_{1-x}Sr_xRuO_3$ solid solutions has been published so far. In the present study, $Ca_{1-x}Sr_xRuO_3$ compounds were synthesized by a solid-state

* Corresponding author. Tel.: +81 22 2152106; fax: +81 22 2152107.
E-mail address: turong@imr.tohoku.ac.jp (R. Tu).

0925-8388/$ – see front matter © 2012 Elsevier B.V. All rights reserved.
doi:10.1016/j.jallcom.2012.01.150

Table 1
Comparison of $CaRuO_3$ and $SrRuO_3$ in crystal structure, electrical, thermal and thermoelectric properties.

	Crystal structure	Lattice parameter (nm)	σ (S m^{-1}), 300–1100 K	κ (W m^{-1} K^{-1}), 300–1100 K	S (mV K^{-1}), 300–1100 K	ZT, 300–1100 K
$CaRuO_3$	Orthorhombic *Pnma*	a = 0.5536 b = 0.7673 c = 0.5364	2×10^5–1×10^5	3.5–4.0	30–35	0.015–0.03
$SrRuO_3$	Orthorhombic *Pnma*	a = 0.5573 b = 0.7856 c = 0.5538	3×10^5–2×10^5	4.5–6.0	30–35	0.02–0.03

reaction and compacted by SPS, and the effect of the composition on the crystal structure, electrical conductivity (σ), thermal conductivity (κ), Seebeck coefficient (S) and dimensionless figure-of-merit (ZT) was investigated.

2. Experimental procedures

$Ca_{1-x}Sr_xRuO_3$ compounds were synthesized by a solid-state reaction using $CaCO_3$ (99.5%), $SrCO_3$ (99.5%) and RuO_2 (99.99%) in various molar ratios of x = 0–1.0. The powders were pressed into pellets and calcined at 1273 K for 43.2 ks in air by a conventional electric furnace. After the calcined pellets were crushed, the resulting powder was compacted by SPS at 1523 K for 0.18 ks in a vacuum at a load of 80 MPa. The compacted body was cut to 2 mm × 2 mm × 10 mm for measurement of electrical conductivity and Seebeck coefficient by a d.c. 4-probe method and a thermoelectric power (ΔE)–temperature difference (ΔT) method, respectively. A disk-shaped specimen 10 mm in diameter and 1 mm in thickness was employed to measure thermal conductivity by a laser flash method (ULVAC TC-7000). All measurements were conducted from room temperature (*RT*) to 1023 K. The crystal phases were identified by X-ray diffraction (XRD, Rigaku Geigerflex). The lattice parameters were calculated by a least-squares method in which the standard deviation of d-values was less than 0.02%. The composition of the specimens was examined by electron probe microanalysis (EPMA, JEOL JXA-8621MX). The density (d) was determined by the Archimedes' method.

3. Results and discussion

Fig. 1 shows XRD patterns of SPS-compacted $Ca_{1-x}Sr_xRuO_3$ bodies at x = 0–1.0. $CaRuO_3$ and $SrRuO_3$ in a single phase were obtained at x = 0 and 1.0, respectively. All specimens at x = 0.1–0.9 were a single phase of the solid solution of $CaRuO_3$ and $SrRuO_3$. With increasing x, the peaks of $CaRuO_3$ shifted continuously to low angles. Peaks of (2 0 0) and (0 0 2) around $2\theta = 32^\circ$ of $Ca_{1-x}Sr_xRuO_3$ disappeared at $x > 0.6$ since the composition is close to that of $SrRuO_3$. The experimental results were coincident with the JCPDS cards of $CaRuO_3$ and $SrRuO_3$.

The composition dependence of the lattice parameters of $Ca_{1-x}Sr_xRuO_3$ compacted bodies in the present study was almost the same as those reported in the literature [14]. With increasing x, the length of b and c axes increased from 0.7714 to 0.7828 nm and from 0.5403 to 0.5543 nm, respectively. However, the length of the a axis slightly decreased with increasing x up to 0.6 and then slightly increased. The unit cell volume increased continuously with increasing x. Kobayashi et al. have also reported the same dependence of lattice parameters vs. x. The continuous change of the lattice parameters from x = 0 to 1.0 indicated the whole solid solution range between $CaRuO_3$ and $SrRuO_3$.

Fig. 2 shows the relative densities of $Ca_{1-x}Sr_xRuO_3$ compacted bodies. The densities at $x < 0.4$ were less than 80% of the theoretical density and increased with increasing x, being 95% at x = 0.9. In our previous studies, $CaRuO_3$ (about 80% at 1523 K) showed poor sinterability as compared with that of $SrRuO_3$ (about 95% at 1523 K) [20].

Fig. 3 demonstrates the fracture microstructure of $Ca_{1-x}Sr_xRuO_3$ compacted bodies at x = 0.2, 0.4, 0.6 and 0.9. At x = 0.2–0.6, many pores were observed (Fig. 3(a)–(c)), whereas the specimen at x = 0.9

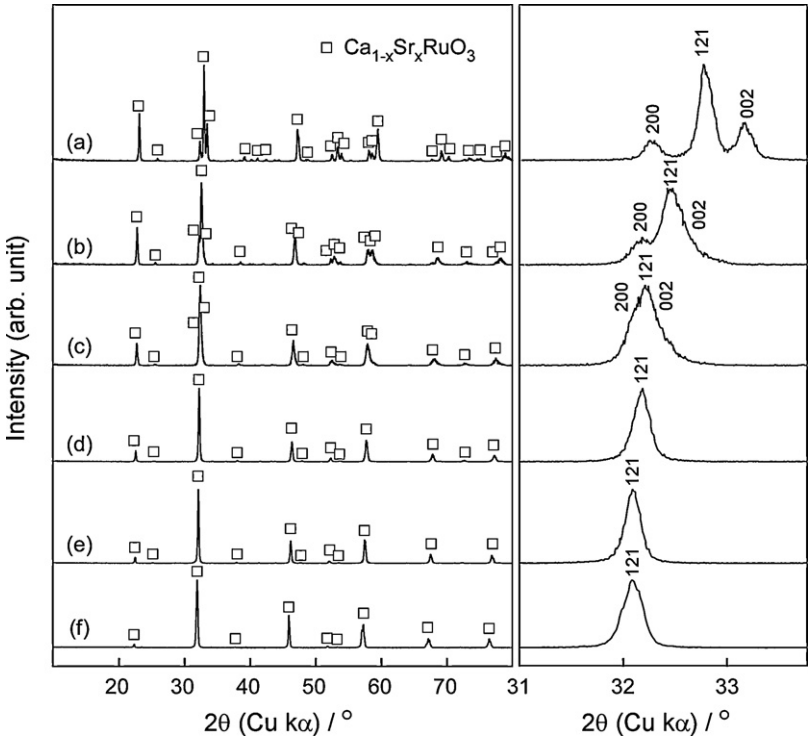

Fig. 1. XRD patterns of SPS-compacted $Ca_{1-x}Sr_xRuO_3$ bodies at x = (a) 0, (b) 0.2, (c) 0.4, (d) 0.6, (e) 0.8 and (f) 1.0.

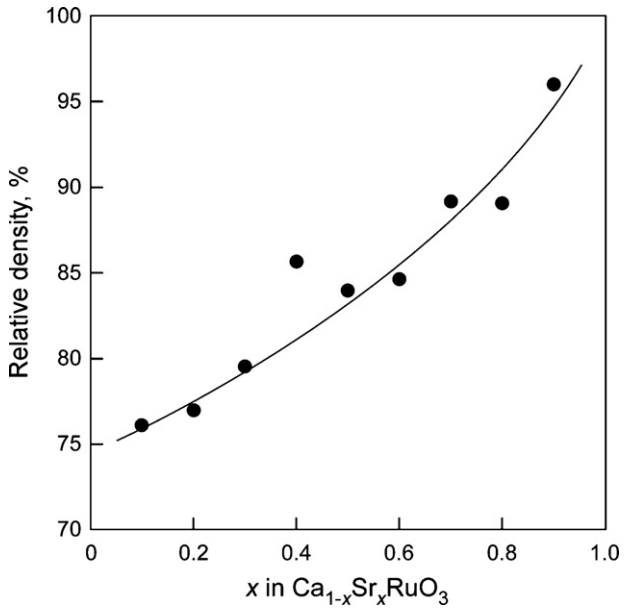

Fig. 2. Relative densities of $Ca_{1-x}Sr_xRuO_3$ compacted bodies by SPS.

had a dense microstructure (Fig. 3(d)). Grain size increased with increasing x from less than 1 μm at $x = 0.2$ to 1–2 μm at $x = 0.4$–0.6 to 1–3 μm at $x = 0.9$.

Fig. 4(a) presents the temperature dependence of electrical conductivity (σ) of $Ca_{1-x}Sr_xRuO_3$ compacted bodies. The σ at all compositions decreased with increasing temperature, showing metallic conduction [14]. Since the σ of $CaRuO_3$ is lower than that of $SrRuO_3$ due to the more greatly distorted orthorhombic structure, the σ of $Ca_{1-x}Sr_xRuO_3$ compacted bodies might have been expected to increase with increasing x. However, the σ at $x = 0.2$ was the highest and that at $x = 0$ ($CaRuO_3$) was the lowest. Furthermore, the σ is depended on the relative density, which increased with increasing x as shown in Fig. 2. The electrical conductivity of fully dense $Ca_{1-x}Sr_xRuO_3$ (σ_c) is compensated by the Maxwell–Eucken's equation (1) [21,22], as shown in Fig. 4(b).

$$\sigma = \sigma_c \times \frac{1-p}{1+\beta p} \quad (1)$$

where p is the porosity, σ the measured electrical conductivity with porosity (p), and β the constant number determined by the conditions of the pores. According to the researches by Asamoto et al. [23] and Biancheria [24], the value of β is 0.5 for relative density of 90–100%, 1.0 for 85–90%, 1.4 for 80–85% and 1.6 for 75–80%. The compensated electrical conductivity of the $Ca_{1-x}Sr_xRuO_3$ solid solution is higher than that of $CaRuO_3$ and $SrRuO_3$. The σ_c of $SrRuO_3$ showed almost the same values with those reported by Maekawa et al. [25], which decreased from 3×10^5 to 1.4×10^5 S m^{-1} at 300–1000 K. The σ_c at $x = 0.2$ showed the highest values. According to the study by Kobayashi [14], the average inter-atomic distance of Ru–O is 0.19905, 0.19892, 0.19913, 0.19964, 0.19920, 0.19936 and 0.19841 nm at $x = 0$, 0.2, 0.4, 0.5, 0.6, 0.8 and 1.0, respectively. The Ru–O distance at $x = 0.2$ is the shortest, except at $x = 1.0$. Since the electrical conduct in $Ca_{1-x}Sr_xRuO_3$ is mainly contributed by the RuO_6 octahedra, the high σ_c at $x = 0.2$ might have been caused by the short Ru–O distance.

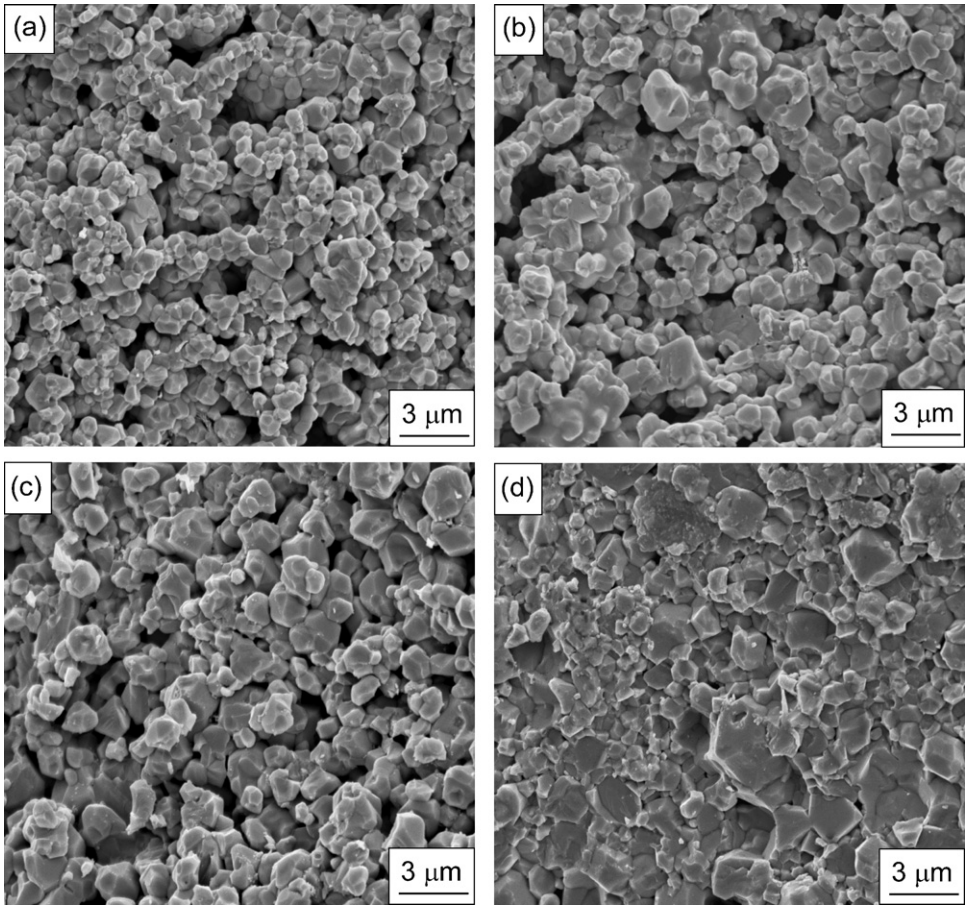

Fig. 3. Fracture microstructure of $Ca_{1-x}Sr_xRuO_3$ compacted bodies at $x =$ (a) 0.2, (b) 0.4, (c) 0.6 and (d) 0.9.

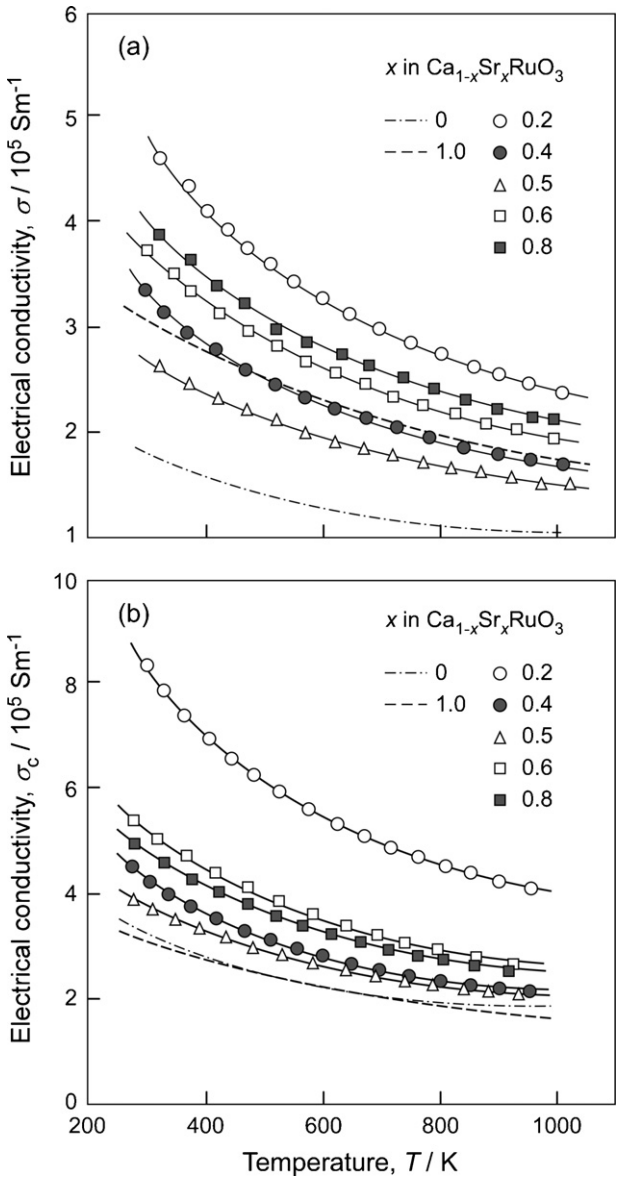

Fig. 4. Temperature dependence of (a) measured and (b) Maxwell–Eucken's equation compensated electrical conductivity of $Ca_{1-x}Sr_xRuO_3$ compacted bodies.

Fig. 5 depicts the composition dependence of electrical conductivity of polycrystalline $Ca_{1-x}Sr_xRuO_3$ compacted bodies at room temperature in the present study and that reported by Kobayashi et al. [14] The σ at $x = 0.1$ to 0.4 and 0.6 to 0.9 were higher than those of $CaRuO_3$ and $SrRuO_3$. However, the σ at $x = 0.5$ was intermediate between those of $CaRuO_3$ and $SrRuO_3$. This trend was almost the same as that reported by Kobayashi et al. [14]; however, the values in the present study were 3 to 4 times greater than those of Kobayashi et al., probably due to higher density by SPS. The σ at $x = 0.2$ showed the highest values, i.e., 4.7×10^5 S m^{-1} at *RT*. Kobayashi et al. suggested that the change of σ of $Ca_{1-x}Sr_xRuO_3$ with x may be closely related to the crystal structure [14]. In the unit cell of $CaRuO_3$ and $SrRuO_3$, there are 8 short bonds and 4 long bonds of Ca(Sr)—O. Kobayashi et al. reported that the length of the 8 short bonds may slightly increase and those of the 4 long bonds may significantly decrease with increasing x. Furthermore, the angle of Ru—O—Ru may increase with increasing x, indicating that the length of the Ru—O—Ru bond may decrease with increasing x [14]. Such complicated behavior of crystal distortion by substitution might have caused the non-monotonous change of σ.

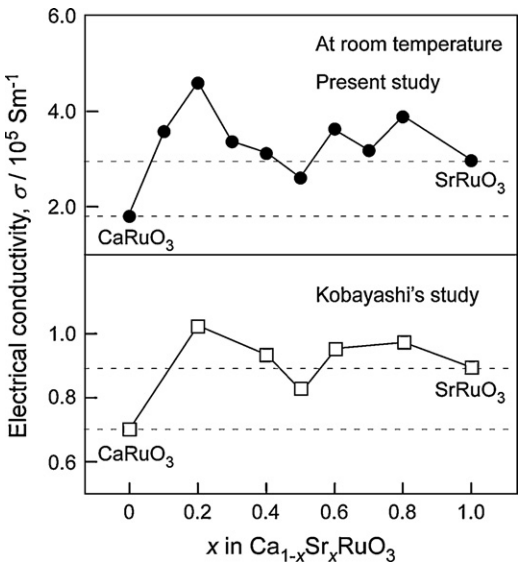

Fig. 5. Composition dependence of electrical conductivity of $Ca_{1-x}Sr_xRuO_3$ compacted bodies at room temperature in the present study and that reported by Kobayashi et al. [14].

Fig. 6 shows the temperature dependence of Seebeck coefficient (S) of $Ca_{1-x}Sr_xRuO_3$ compacted bodies. The S for any composition showed positive values, exhibiting a *p*-type. The S was almost independent of composition and temperature, around 30–40 μV K^{-1}. In the literature, the S of $CaRuO_3$ and $SrRuO_3$ was around 35 μV K^{-1} reported by Annamalai et al. [26] and Maekawa et al. [25], respectively, which is consistent with our results.

Fig. 7(a) shows the temperature dependence of thermal conductivity (κ) of $Ca_{1-x}Sr_xRuO_3$ compacted bodies. The κ at any composition increased from 2.0 to 6.0 W m^{-1} K^{-1} with increasing temperature from *RT* to 1000 K. The κ at $x = 1.0$ ($SrRuO_3$) was the highest, which is lower than that reported by Maekawa et al. (6–8 W m^{-1} K^{-1} at 300–1200 K) [25]. The κ at $x = 0.2$ was lower than those of the end members in the whole temperature ranges. The lowest κ was observed at $x = 0.2$, may be caused by the highest porosity. In order to eliminate the effect of porosity on the thermal conductivity, Maxwell–Eucken's equation (1), where σ is replaced

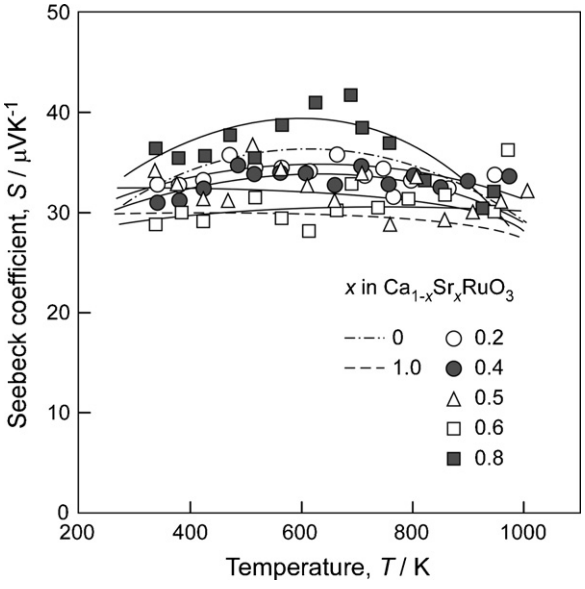

Fig. 6. Temperature dependence of Seebeck coefficient of $Ca_{1-x}Sr_xRuO_3$ compacted bodies.

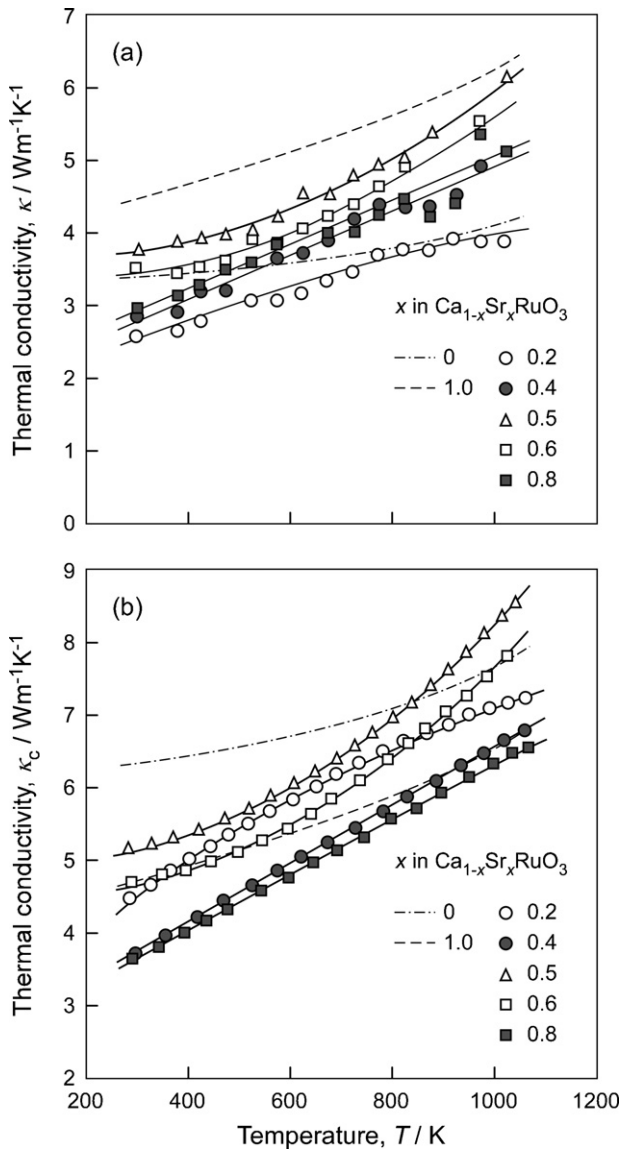

Fig. 7. Temperature dependence of (a) measured and (b) Maxwell–Eucken's equation compensated thermal conductivity of $Ca_{1-x}Sr_xRuO_3$ compacted bodies.

by κ, was applied to calculate the thermal conductivity of fully dense $Ca_{1-x}Sr_xRuO_3$ (κ_c), which is shown in Fig. 7(b). Different from the lowest κ at $x = 0.2$ in Fig. 7(a), κ_c shows the lowest value at $x = 0.8$. The average inter-atomic distance of Ru–O at $x = 0.8$ is the largest, except at $x = 0.5$ [14]. The large inter-atomic distance might have been related to the lowest κ_c at $x = 0.8$.

Fig. 8 shows the temperature dependence of the dimensionless figure-of-merit (ZT) of $Ca_{1-x}Sr_xRuO_3$ compacted bodies calculated from equation (2)

$$ZT = \frac{S^2\sigma T}{\kappa} \quad (2)$$

The ZT was almost independent of temperature and composition. The ZT at all compositions was higher than those of end members due to the combination of higher electrical conductivity and lower thermal conductivity. Due to the highest electrical conductivity and the lowest thermal conductivity at $x = 0.2$, furthermore the composition independence of Seebeck coefficient, the highest ZT was 0.07 at $x = 0.2$ and 600 K. This value was twice those of the end members, i.e., 0.025. Kawano et al. prepared solid solution of $Co_{3-x}Ru_xO_y$ ($0.5 \le x \le 0.7$, $y = 3.8$–3.9) from Co_3O_4

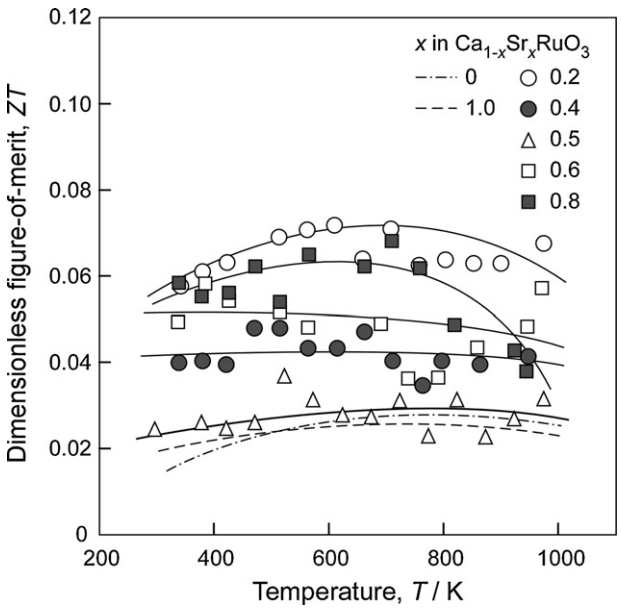

Fig. 8. Temperature dependence of dimensionless figure-of-merit (ZT) of $Ca_{1-x}Sr_xRuO_3$ compacted bodies.

and RuO_2 powders by solid-state reaction at 1173–1273 K in air [27]. Comparing to $Ca_{1-x}Sr_xRuO_3$, $Co_{3-x}Ru_xO_y$ had higher Seebeck coefficient (200 $\mu V K^{-1}$ at 300 K) and lower thermal conductivity (1.0 $W K^{-1} m^{-1}$ at 300 K). However, as the electrical conductivity of $Co_{3-x}Ru_xO_y$ was 1 order lower than that of $Ca_{1-x}Sr_xRuO_3$, the highest ZT was 0.024 at 973 K, which is much lower than that of $Ca_{1-x}Sr_xRuO_3$.

4. Conclusions

$Ca_{1-x}Sr_xRuO_3$ solid solution bodies were prepared by SPS. The lattice parameters changed continuously in the whole range of x. The relative densities increased from 75 to 95% with increasing x. The σ of all compositions showed metallic conduction and was mostly higher than those of the end members. The σ at $x = 0.2$ showed the highest value, i.e., 4.7×10^5 S m^{-1} at room temperature. The S of all specimens showed positive values, exhibiting a p-type. The S was almost independent of composition and temperature, around 30–40 $\mu V K^{-1}$. The κ at $x = 0.2$ was lower than those of the end members in the whole temperature range. The lowest κ was observed at $x = 0.2$. The highest ZT was 0.07 at $x = 0.2$ and 600 K.

Acknowledgments

The authors are grateful to the Global COE Program, Materials Integration, JSPS Asian CORE program, Furuya Metal Co., Ltd. and Lonmin Plc. for financial support.

References

[1] I. Felner, I. Nowik, I. Bradaric, M. Gospodinov, Phys. Rev. B 62 (2000) 11332.
[2] K. Char, M.S. Colclough, T.H. Geballe, K.E. Myers, Appl. Phys. Lett. 62 (1993) 196.
[3] K. Gurunathan, N. Vyawahare, D.P. Amalnerkar, J. Mater. Sci.: Mater. Electron. 16 (2005) 47.
[4] C. Mallika, O.M. Sreedharan, J. Alloys Compd. 177 (1991) 273.
[5] C. Mallika, O.M. Sreedharan, J. Alloys Compd. 191 (1993) 219.
[6] A. Banerjee, R. Prasad, V. Venugopal, J. Alloys Compd. 353 (2003) 263.
[7] X.Y. Zhang, Y.J. Chen, Z.Y. Li, J. Alloys Compd. 459 (2008) 51.
[8] S. Middey, P. Mahadevan, D.D. Sarma, Phys. Rev. B 83 (2011) 014416.
[9] N. Keawprak, R. Tu, T. Goto, Mater. Trans. 48 (2007) 1529.
[10] N. Keawprak, R. Tu, T. Goto, Key Eng. Mater. 352 (2007) 251.
[11] N. Keawprak, R. Tu, T. Goto, Mater. Sci. Forum 561–565 (2007) 595.
[12] N. Keawprak, R. Tu, T. Goto, Mater. Trans. 49 (2008) 600.

[13] M.V. Rama Rao, V.G. Sathe, D. Sornadurai, B. Panigrahi, T. Shripathi, J. Phys. Chem. Solids 62 (2001) 797.
[14] H. Kobayashi, M. Nagata, R. Kanno, Y. Kawamoto, Mater. Res. Bull. 29 (1994) 1271.
[15] P.B. Allen, H. Berger, O. Chauvet, L. Forro, T. Jarlborg, A. Junod, B. Revaz, G. Santi, Phys. Rev. B 53 (1996) 4393.
[16] R.J. Bouchard, J.L. Gillson, E.I. du Pont de Nemours, Mater. Res. Bull. 7 (1972) 873.
[17] L. Capogna, A.P. Mackenzie, R.S. Perry, S.A. Grigera, L.M. Galvin, P. Raychaudhuri, A.J. Schofield, Phys. Rev. Lett. 88 (2002) 076602–76611.
[18] M. Wissinger, D. Fuchs, L. Dieterle, H. Leiste, R. Schneider, D. Gerthsen, H.V. Löhneysen, Phys. Rev. B 83 (2011) 144430.
[19] I.M. Gat-Malureanu, J.P. Carlo, T. Goko, A. Fukaya, T. Ito, P.P. Kyriakou, M.I. Larkin, G.M. Luke, P.L. Russo, A.T. Savici, C.R. Wiebe, K. Yoshimura, Y.J. Uemura, Phys. Rev. B 84 (2011) 224415.
[20] N. Keawprak, R. Tu, T. Goto, Mater. Sci. Eng. B 161 (2009) 71.
[21] A. Eucken, Forschung 11 (1940) 6.
[22] J. Adachi, K. Kurosaki, M. Uno, S. Yamanaka, J. Alloys Compd. 432 (2007) 7.
[23] R.R. Asamoto, F.L. Anselin, A.E. Conti, J. Nucl. Mater. 29 (1969) 67.
[24] A. Biancheria, Trans. Am. Nucl. Soc. 9 (1966) 15.
[25] T. Maekawa, K. Kurosaki, H. Muta, M. Uno, S. Yamanaka, J. Alloys Compd. 387 (2005) 56.
[26] S. Annamalai, I. Vidensky, I.L. Pegg, B. Dutta, J. Mater. Sci. 43 (2008) 4996.
[27] T. Kawano, J. Takahashi, T. Okutani, T. Yamada, H. Yamane, J. Alloys Compd. 468 (2009) 447.